Use of patient-derived tumor organoids from head and neck squamous cell carcinoma for the evaluation of the differential effect of carbon ions over X-rays

Marion Perréard, Romane Florent, Jordane Divoux, Vianney Bastit, Lucie Lecouflet, Guillaume Desmartin, Sterenn Guillemot, Léonie Ibazizene, Nicolas Elie, Emilie Brotin, et al.

Radiotherapy and Oncology 210 (2025) 111026

Contents lists available at ScienceDirect

Radiotherapy and Oncology

journal homepage: www.thegreenjournal.com

Original Article

Use of patient-derived tumor organoids from head and neck squamous cell carcinoma for the evaluation of the differential effect of carbon ions over X-rays

Marion Perréard [a,b,*], Romane Florent [c], Jordane Divoux [a,c,d], Vianney Bastit [a,b], Lucie Lecouflet [c,d], Guillaume Desmartin [c,d], Sterenn Guillemot [a], Léonie Ibazizene [a], Nicolas Elie [e], Emilie Brotin [f], Laurent Poulain [a,c,d], Emmanuel Babin [a,b], Juliette Thariat [g,h], François Chevalier [i], Louis-Bastien Weiswald [a,c,d,*]

[a] Université de Caen Normandie, INSERM U1086 ANTICIPE (Interdisciplinary Research Unit for Cancers Prevention and Treatment), BioTICLA laboratory (Precision medicine for ovarian cancers), Caen, France
[b] Caen University Hospital, Department of Head and Neck Surgery, Caen, France
[c] Université de Caen Normandie, PLATON Services Unit, ORGAPRED core facility, Caen, France
[d] UNICANCER, Comprehensive Cancer Center François Baclesse, Caen, France
[e] Université de Caen Normandie, PLATON Services Unit, VIRTUAL'HIS core facility, Caen, France
[f] Université de Caen Normandie, PLATON Services Unit, ImpedanCELL core facility, Caen, France
[g] UNICANCER, Comprehensive Cancer Center François Baclesse, Department of Radiation Oncology, Caen, France
[h] Université de Caen Normandie, Laboratoire de Physique Corpusculaire/IN2P3-CNRS UMR 6534-ARCHADE, Caen, France
[i] Université de Caen Normandie, UMR6252 CIMAP, CEA-CNRS-ENSICAEN, Team Applications in Radiobiology with Accelerated Ions, Caen, France

ARTICLE INFO

Keywords:
Head and neck squamous cell carcinoma
Patient-derived tumor organoids
Carbon ions
X-rays
Hadrontherapy
Organoid forming assay

ABSTRACT

Background and purpose, Conventional radiotherapy, based on the use of X-rays, remains a standard treatment modality for advanced Head and Neck Squamous Cell Carcinoma (HNSCC), either as a standalone approach or in combination with surgery and/or chemotherapy. Despite its widespread use, approximately 50% of HNSCC patients ultimately experience locoregional recurrence, underscoring the critical need to improve the therapeutic efficacy of radiotherapy. Heavy particles such as carbon ions could lead to better efficiency in treating HNSCC with less side effects. Patient-Derived Tumor Organoids (PDTO) are new 3D *in vitro* model close to original tumor. However, cancer cell inactivation and/or death induced by carbon ions have not been assessed on PDTO so far or even compared to X-ray.

Methods and Materials, Five PDTO lines established from HNSCC patients were exposed to carbon ions and to X-rays and their response to treatments were compared using viability assay, cell cycle analysis and a newly designed clonogenic assay named Organoid Forming Assay (OFA).

Results, Viability assays showed a better cell killing effect of carbon ions over X-Rays with a relative biological effect (RBE) ranging from 1.14 to 1.94. OFA revealed a better efficiency of carbon ions over X-rays in a X-ray-resistant PDTO line (RBE at 6.54) compared to a X-ray-sensitive one (RBE at 4.23). These results were confirmed using cell cycle analysis and viability assay.

Conclusions, OFA could be a new alternative assay to evaluate different radiotherapy modalities including carbon ions on PDTO models. These results suggest that PDTO may be used to study effects of carbon ions and carbon ions could overcome radioresistance to photons observed in some patients and lead to improvement in management of HNSCC patients.

Abbreviations: 3D, three-dimensional; ATP, adenosine triphosphate; AUC, area under the curve; BME, basement membrane extract; CFA, colony forming assay; CSC, cancer stem cells; HNSCC, head and neck squamous cell carcinoma; IMRT, intensity-modulated radiotherapy; LET, linear energy transfer; OAR, organs at risk; OBM, organoid basal medium; OCM, organoid culture medium; OFA, organoid forming assay; OTM, organoid treatment medium; PBS, phosphate-buffered saline; PDTO, patient-derived tumor organoids; RBE, relative biological effect.

* Corresponding authors at: INSERM U1086 ANTICIPE (Interdisciplinary Research Unit for Cancer Prevention and Treatment), Comprehensive Cancer Center François Baclesse, 3 Avenue du Général Harris, BP 45026, Caen cedex 05 14 076, France.
E-mail addresses: perreard-m@chu-caen.fr (M. Perréard), lb.weiswald@baclesse.unicancer.fr (L.-B. Weiswald).

https://doi.org/10.1016/j.radonc.2025.111026
Received 31 January 2025; Received in revised form 22 May 2025; Accepted 29 June 2025
Available online 3 July 2025

Introduction

Head and Neck Squamous Cell Carcinoma is an aggressive cancer with more than 50 % of patients being diagnosed at an advanced stage (stage III and IV – AJCC 8th edition) [1]. Curative therapies used are concomitant radiochemotherapy or surgery followed by radiotherapy or radiochemotherapy. Conventional therapy uses photons in intensity-modulated radiotherapy (IMRT), possibly with cisplatin for its synergistic effect. Despite those heavy treatments responsible of major side effects, the recurrence rate is high, approximately 60 % [1]. Current research focuses on the identification effective radiosensitizers or on new modalities of irradiation to improve efficiency of the treatment. No radiosensitizer has yet made it through clinical trials [2]. Heavy particles such as carbon ions could be promising according to their physical and biological properties. Compared to photons, high Linear Energy Transfer (LET) particles allow a better relative biological effect (RBE) associated with a higher precision of deposition of energy thanks to the Bragg Peak. These characteristics conduct to a better sparing of organs at risk (OAR) of hadrontherapy [3]. Those properties could thus lead to better efficiency in treating HNSCC with less side effects to healthy tissues.

Previous studies on carbon ions and HNSCC have been mostly performed on 2D cell lines [4,5]. However, it is widely accepted that most of the cancer cell lines available do not accurately mimic the pathology due to lack of heterogeneity and genetic drift over time [6] and alternatives to animal testing are encouraged at the international level [7]. Three-dimensional (3D) *in vitro* models were introduced in cancer research by radiobiologists as an intermediate model between *in vitro* 2D cancer cell lines and *in vivo* tumors [8]. These models allowed mimicking metabolic gradients of oxygen, nutrients, and waste products, which could strongly modulate the response of cells to treatments in addition to 3D cellular interactions [9]. Few studies have used 3D models of normal tissue (intestinal tissue, cartilage or oral mucosa) [10–12] or 3D HNSCC models to study carbon ions effects, either using ultra-low attachment plates [13], extracellular matrix [14] or decellularized biological scaffolds [15], but always using commercial malignant cell lines. Patient-Derived Tumor Organoids (PDTO) represent relevant 3D *in vitro* models that recapitulate tumors of origin [16]. The response of PDTO lines derived from HNSCC after exposure to X-rays has been studied using viability assay and first evidence of correlation with clinical response of the patients was demonstrated [17–19]. Nevertheless, effects of carbon ions have not been assessed on PDTO so far or even compared to X-ray.

The aim of this study was first to assess the feasibility of irradiation of HNSCC PDTO with carbon ions and to develop new methods to assess the PDTO response in a more integrative approach. A second objective was to determine the Relative Biological Effectiveness (RBE) of carbon ions in the PDTO lines.

Materials and methods

PDTO culture

PDTO were established and cryopreserved as previously described [20]. The clinical characteristics of the patients from which PDTO models used in this paper were derived are described in Table 1, as well as the sensitivity/resistance to X-rays of PDTO selected for this study. PDTO culture is described in detail in Supplementary Methods.

Irradiations

Preparation for irradiation

PDTO were collected in cold OBM-BSA (organoid basal medium supplemented with 1 % Bovine Serum Albumin (BSA)), pelleted at 200 g for 2 min, resuspended in OTM (organoid treatment medium, corresponding to organoid culture medium (OCM) lacking Primocin, Y-27632 and N-acetylcysteine), counted and distributed in 1.5 mL polypropylene tube (Eppendorf). For viability assay, tubes contained 4500 PDTO in 1000 µL, for cell cycle analysis 4000 PDTO in 1000 µL, and for clonogenic assay 300 PDTO in 300 µL.

Irradiations

PDTO were irradiated with X-Rays at the physical dose of 0, 2, 4, 8, 10 and 20 Gy in a benchtop compact cabinet X-ray cell irradiator, Faxitron CellRad (X-Ray source, 130 kV, 5 mA, copper filter, at a dose rate of 2 Gy/min).

PDTO were irradiated with carbon ions at 0, 2, 4 and 10 Gy. Carbon ion irradiations were performed using the high-energy beam line (IRABAT) at the Grand Accélérateur National d'Ions Lourds (GANIL, Caen, France). The calibrations and dosimetry were done by by CIMAP (Centre de Recherche sur les Ions, les Matériaux et la Photonique) as previously described [21]. Carbon Ions (95 MeV/a, < 0.1nA) were used in association with a 16.9 mm PMMA degrader, in order to reach a LET of 73,2 keV/µm. With this LET condition, the depth in water of the beam before Bragg peak is about 2.4 mm, which guarantees PDTO irradiation. Irradiations were performed at a dose rate of 2 Gy/min, the mean fluency was about 2,85 e^{+05} ions.cm^{-2}.s^{-1}. PDTO were irradiated at the physical dose of 0, 2, 4 and 10 Gy.

Evaluation of response to radiotherapy

Viability assay

Following irradiation, PDTO were pelleted (200 g, 2 min), resuspended in 2 % Cultrex Reduced Growth Factor Basement Membrane Extract, Type 2 (BME2)/OTM, and 200 PDTO per well were seeded in 200 µL in a previously coated (1:1 OTM/BME2) white clear bottom 96-well plates (Greiner) in triplicate. Plates were transferred to a humidified 37 °C/5% CO2 incubator. PDTO morphology was monitored using IncuCyte S3 (Sartorius). Media was changed after 5 days. Ten days later, ATP levels were measured by CellTiter-Glo 3D assay (Promega) and luminescence was quantified using GloMax (Promega). Viability curves were designed using GraphPad Prism software (version 9.2.0). The area under the curve (AUC) was computed for each PDTO model.

Cell cycle analysis

After irradiation, PDTO were pelleted (200 g, 2 min), resuspended in 2 % BME2/OTM, and 4000 PDTO per well were seeded in 2 mL volume in previously coated (1:1 OTM/BME2) 6-well plates (Nunc). Plates were transferred to a humidified 37 °C/5% CO2 incubator. Media was changed after 5 days. After 10 days, PDTO were collected with cold

Table 1
Clinical characteristics of HNSCC patients from which PDTO models were derived. RT, radiotherapy, CT, chemotherapy.

	Previous Head and Neck RT	Tumor localization	HPV+	Post-operative RT	Post-operative CT	Clinical status at 24 months	Response of PDTO to X-Rays
HN005	No	Larynx	No	**Yes**	No	Remission	Sensitive
HN032	No	Oropharynx	**Yes**	**Yes**	**Cisplatin**	Remission	Sensitive
HN052	No	Oropharynx	No	No	No	**Progression**	**Resistant**
HN065	**Yes**	Hypopharynx	No	No	No	Remission	Sensitive
HN099	**Yes**	Oropharynx	No	No	No	**Progression**	**Resistant**

OBM-BSA, centrifuged (200 g, 2 min) and incubated with TrypLE Express for up to 15 min at 37 °C. After dissociation, cells were washed with PBS (Phosphate-Buffered Saline), fixed with ethanol 70 % and stored at −20 °C. Cells were then centrifuged (2700 g, 5 min) and incubated for 30 min at 37 °C in PBS, to allow the release of low-molecular weight DNA. Cell pellets were stained with a solution composed by 600 μg/mL of RNAse A (Fisher Scientific) and 50 μg/mL of propidium iodide (Fisher Scientific) diluted in PBS. Samples were analyzed using a Gallios flow cytometer (Beckman-Coulter) and cell cycle distribution and sub-G1 fraction were determined using Kaluza software (Beckman-Coulter).

Organoid forming assay (OFA)

Following irradiation, PDTO were pelleted (200 g, 2 min), and incubated with TrypLE Express for up to 15 min at 37 °C. After dissociation, cells were centrifuged (430 g, 5 min), suspended in organoid culture medium (OCM), and plated in 50 μl drop of 70 % BME2 in pre-warmed 24-well plates. After polymerization (37 °C, 5 % CO2, 15 min), each drop was immersed with OCM. Plates were transferred to a humidified 37 °C/5% CO2 incubator. Formation of PDTO was monitored using IncuCyte S3 (Sartorius) for 20 days every 24 h. The sequence of images acquired was analysed using Fiji software [22]. First, the images were adjusted to ensure proper alignment throughout the sequence using the Linear Stack Alignment plugin [23]. Next, the images were processed with mathematical morphology operators and Fiji's automatic moment thresholding method. The resulting binary images were used to measure the area occupied by the PDTO in the drop, allowing for the calculation of the percentage of the drop's surface occupied by the PDTO line. Only objects with a minimum surface of 10 μm^2 were considered as PDTOs and included in the analysis, in order to exclude cellular debris and non-specific background signals. The image processing code is publicly available at the following link, https://git.unicaen.fr/nicolas.elie/process_incucyte. Curves were designed using GraphPad Prism software (version 9.2.0).

RBE

RBE was calculated as the ratio of X-rays values to carbon ions values with AUC of the viability curve measured after 10 days or with the percentage of the drop's surface occupied by the PDTO line after 10 days.

Results

To assess the best delay before the readout of the end-point viability test, we first compared the results 5, 10, 15 and 20 days post-irradiation on one PDTO line (**Supplementary Fig. 1**). After irradiation with X-Rays, we observed a higher variability of response between replicates after 5 days compared to other times. Following irradiation with carbon ions, the viability assay showed similar response after 5, 10, 15 or 20 days. We then exposed five PDTO lines to increased doses of carbon ions and X-rays and analyzed the viability response 10 days post-irradiation (Fig. 1). For the X-ray resistant PDTO lines HN052 and HN099 (viability at 10 Gy above 50 %), viability dropped below 50 % after exposure to 10 Gy carbon ions. For HN005 and HN065, the viability was above 50 % at 4 Gy after X-rays and below 50 % at 4 Gy after carbon ions. For HN032, a PDTO line with high sensitivity to X-rays, the viability at 2 Gy was above 50 % for X-rays but below 50 % for carbon ions. Cell survival after 10 days was thus decreased with carbon ions compared to X-rays in all PDTO lines, showing higher efficiency of carbon ions over X-Rays. We evaluated the induction and repair kinetics of DNA damage in HN005 PDTO following exposure to carbon ions and X-rays **(Supplementary Fig. 2)**. Immunofluorescence staining for RAD51 and γH2AX was performed to monitor DNA double-strand break formation and homologous recombination-mediated repair, respectively. A transient increase in RAD51 foci was observed 2 h after X-ray exposure, returning to baseline levels by 8 h, in parallel with a reduction in γH2AX foci, indicating effective DNA repair. In contrast, carbon ion exposure resulted in a pronounced and sustained accumulation of both RAD51 and γH2AX foci at 2 h, with only a slight decrease observed at 8 h. These results suggest that DNA damage induced by carbon ions may be more extensive and/or more difficult to repair than that caused by X-rays. In the X-ray sensitive PDTO line HN065, carbon ions displayed a moderately higher effect on viability compared to X-rays. Interestingly, in the most radioresistant PDTO line HN099, carbon ions induced a stronger decrease of viability compared to X-Rays. These data were further supported by the morphological appearance of PDTOs at the end of the experiment, while PDTOs from line HN099 continued to grow after exposure to 10 Gy of X-rays, they showed signs of disintegration at the same dose of carbon ions (**Supplementary Fig. 3**).

As for the three other PDTO lines, more various responses to X-rays and to carbon ions were observed but always with a higher cell killing effect of carbon ions (**Supplementary Fig. 4**). We calculated the RBE of carbon ions over X-rays for the different PDTO lines using the ratio of AUC from the dose–response curve (Fig. 1). The mean of the RBE for the 5 lines was 1.49, ranging from 1.14 to 1.94. Interestingly, the highest RBE (1,94) was calculated for the X-ray most resistant PDTO line HN099 while the X-ray most sensitive PDTO line HN032 displayed the lowest RBE (1,14).

In order to adapt the conventional colony forming assay to PDTO culture, we developed the Organoid Forming Assay (OFA) which aimed at evaluating the capacity of tumor cell to grow as PDTO following irradiation. We also developed a method to monitor the area occupied by PDTO over time to be able to quantify effects of treatment in real-time (see material and methods, **Supplementary Fig. 5**). Using this method, we observed that PDTO line HN065 maintained a capacity to produce PDTO from single cells after irradiation at 2 Gy with X-Rays. The ability to generate PDTO from single cells was drastically decreased after 2 Gy of carbon ions and almost null after 10 Gy of X-rays and carbon ions (Fig. 2**A and C**). These results confirmed that the HN065 line was sensitive to X-rays and even more sensitive to carbon ions. On the other hand, the PDTO line HN099 maintained a capacity to produce PDTO from single cells following irradiation at 2 Gy and 10 Gy with X-Rays, in accordance with its X-ray resistant status. Following exposure to carbon ions, the ability to generate PDTO from single cells was lower at 2 Gy than without irradiation and almost null at 10 Gy (Fig. 2**B and D**). These results confirmed that the PDTO line HN099 was resistant to X-Rays while its exposure to carbon ions induced notable cancer cell inactivation. We calculated the RBE of carbon ions over X-rays using the surface of the drop occupied by PDTO at 10 days (Fig. 2). The RBE from OFA for the radiosensitive PDTO line HN065 was at 3.72 at 2 Gy and 4.23 at 10 Gy while it was at 3.15 at 2 Gy and reached 6.54 at 10 Gy for the radioresistant PDTO line HN099.

Analysis of cell cycle distribution 10 days post-irradiation revealed that the sub-G1 population, including dead and/or apoptotic cells, was increased in a dose-dependent manner in HN065 line after exposure to X-rays and carbon ions (7.88 % and 10.79 % at 2 Gy, 49.91 % and 40.5 % at 10 Gy, respectively) (Fig. 3**, Supplementary Fig. 6**). We also observed a slight increase of G2-M proportion at 10 Gy following X-rays and carbon ions (6.83 % and 8.99 % at 2 Gy, 13.44 % and 12 % at 10 Gy, respectively) suggesting a partial blockage at G2-M phase for both conditions. On the other hand, the irradiation with X-rays at 2 and 10 Gy or the irradiation with carbon ions at 2 Gy had no effect on the cell cycle distribution in HN099 cells with a sub-G1 population between 3.35 % and 4.81 % (Fig. 3**, Supplementary Fig. 6**). Only a dose of 10 Gy with carbon ions induced an increase of the sub-G1 population to 31.4 %.

Discussion

We exposed PDTO lines to carbon ions and X-rays and assessed their response to those modalities of radiotherapy using various assays. We selected day 10 post-irradiation as the optimal timepoint for readout, based on preliminary experiments showing reduced variability between

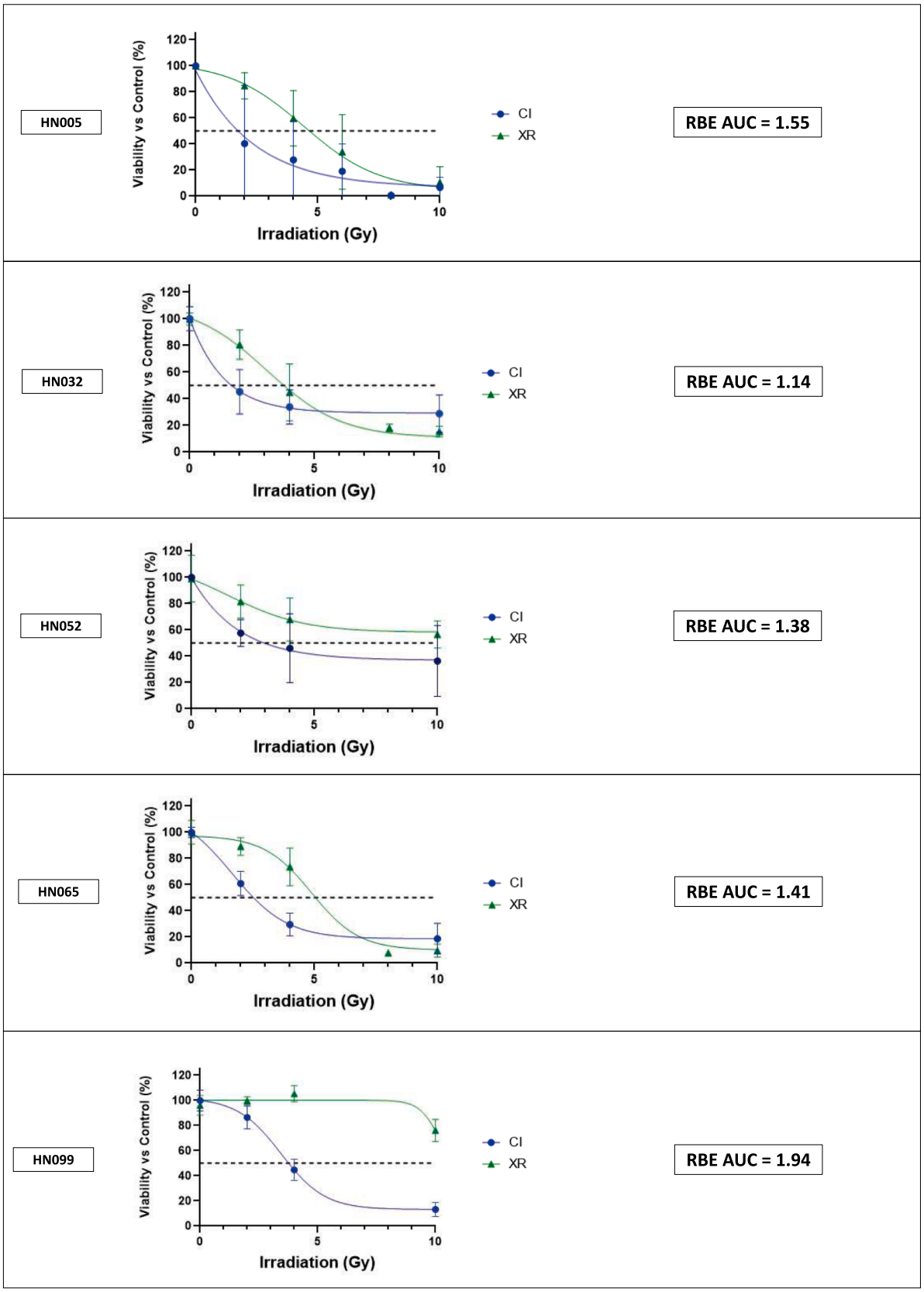

Fig. 1. Comparison of the response of HNSCC PDTO lines to carbon ions and X-Rays using viability assay. Dose-response curves were plotted using viability assay performed 10 days following exposure of 5 PDTO lines to increasing doses of carbon ions or X-rays. Each curve represents the average of two or three experiments (respective AUC available in Supplementary Fig. E2). Relative Biological Effect (RBE) were calculated as the ratio of Area Under Curve (AUC) of XR experiments to those of CI experiments. CI, Carbon Ions, XR, X-Rays.

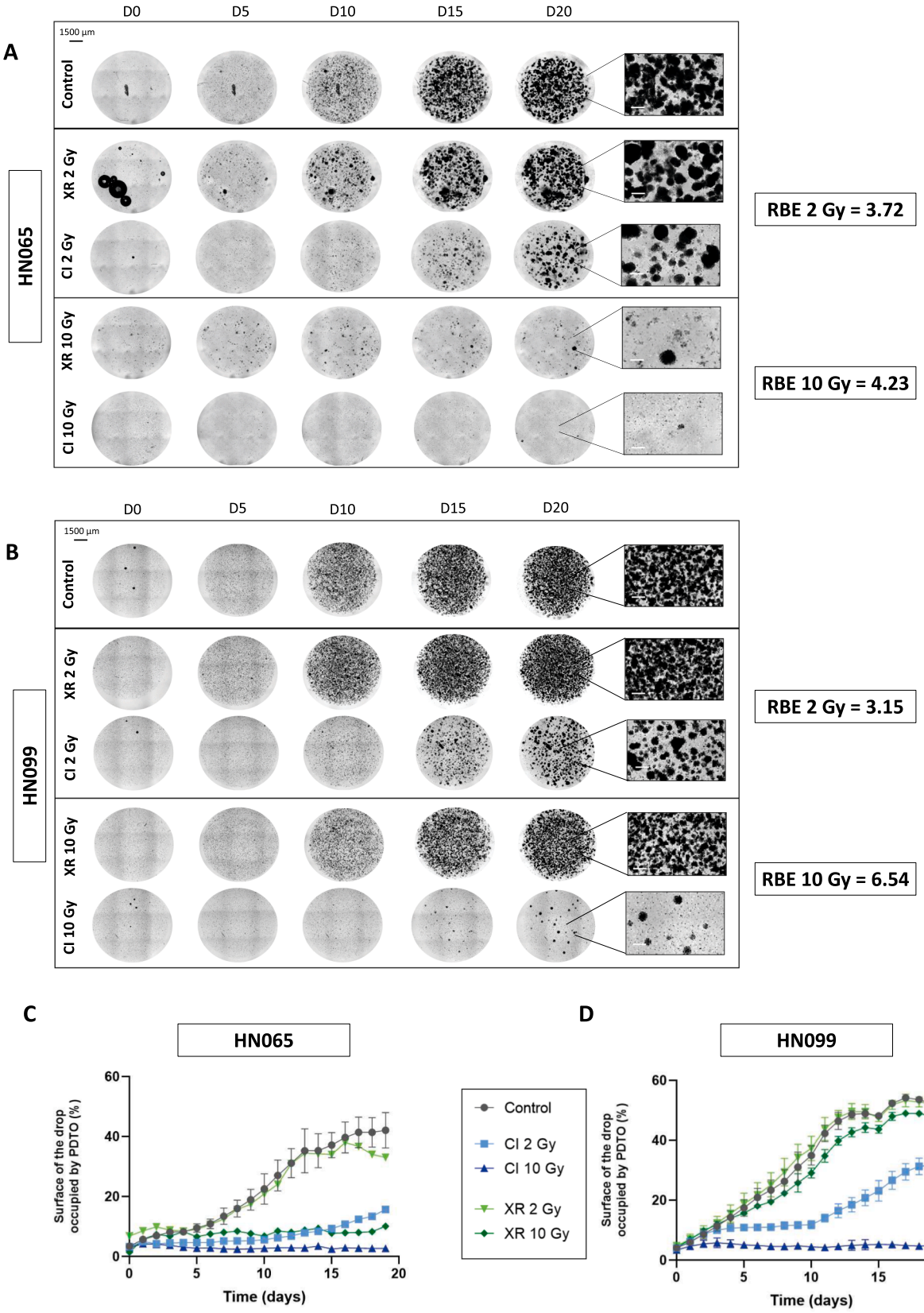

Fig. 2. Comparison of the response of HNSCC PDTO lines to carbon ions and X-Rays using Organoid Forming Assay (OFA). (**A-B**). Representative images of extracellular matrix dome 5, 10, 15 and 20 days post-irradiation with X-rays or carbon ions of X-ray-sensitive PDTO line HN065 (**A**) and X-ray-resistant PDTO line HN099 (**B**). Scale bar = 1500 µm (whole dome) and 300 µm (zoom). RBE were calculated based on the ratio of surface of the drop occupied by PDTO at 10 days. (**C-D**) Quantification of the proportion of the surface of the drop occupied by PDTO lines HN065 (**C**) and HN099 (**D**).

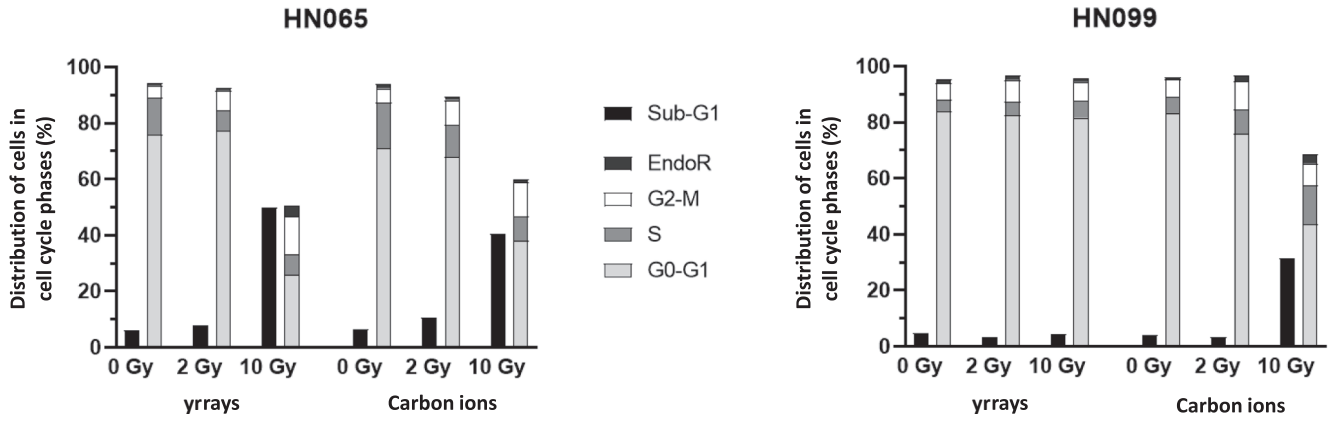

Fig. 3. Analysis of distribution in the cell cycle of HNSCC PDTO cells following exposure to X-ray or carbon ions. Distribution (in percentage) in the cell cycle of the cells of HN065 and HN099 PDTO lines 10 days post-irradiation with X-rays or carbon ions using propidium iodide staining and flow cytometry.

replicates and better capture of long-term effects of radiation (**Supplementary Fig. 1**). Indeed, evaluation at earlier timepoints may miss key consequences of radiation-induced damage, especially in 3D models where sublethal damage can accumulate over time. While we did not directly measure DNA damage, we acknowledge that persistent effects may result from ongoing chromosomal instability in daughter cells that inherit damage, and that only those cells retaining proliferative capacity will eventually repopulate. Similar findings were reported by Roohani et al., who showed in 3D sarcoma models that DNA damage accumulated between day 4 and day 8 after irradiation with protons or photons [14]. Our results are consistent with these observations and emphasize the importance of considering later timepoints to fully assess the efficacy of radiotherapy modalities.

The viability assay showed consistent results across repeated experiments for two PDTO lines (HN065 and HN099), while greater variability was observed in the other three lines. This variation may reflect inherent biological differences between the models, particularly considering the multicellular nature of PDTO and the time elapsed between irradiation sessions, which required multiple passages. Although some variability was noted, carbon ion irradiation tended to result in a stronger cell-killing effect compared to X-rays in all models tested. Clonogenic assay, or colony forming assay, is the gold standard method for assessing radiosensitivity *in vitro* [24] and has already been used to determine the RBE of carbon ions over photons in 2D cells [4,5]. This method analyzes cell viability and quantify reproductive cell survival fraction after treatment with radiation [25]. In this study, we adapted the protocol of the conventional colony forming assay to the culture of PDTO in order to develop the Organoid Forming Assay. The panel of pictures for 20 days showed a dose-dependent decrease of ability of cells to generate PDTO following the different modalities of irradiations (**Supplementary Fig. 5**). The results were quantified by counting the surface occupied by PDTO over the total surface of the extracellular matrix dome to compare the different conditions and were consistent with the previous observations. We chose to focus on the total surface area occupied by PDTOs, as it offers a clear and consistent representation of growth dynamics over time. In contrast, tracking individual PDTO size can be difficult to represent in this context and technically challenging, especially when organoids grow in number and size, often overlapping or merging, which complicates reliable segmentation. A methodology similar to our protocol was described in 2024, with irradiation of PDTO before dissociation and analysis of the surface occupied by the PDTO [26]. Another study investigated the cell inactivation of X-rays on 3D-cultured patient-derived cells of glioblastoma [27] based on the average and standard deviation of an individual colony's area to represent the heterogeneity of growing of the 3D models. Although OFA was performed on only two PDTO lines, the results obtained were globally consistent with the viability assays for these two models despite different RBE values. This can be explained by the fact that the viability assay measures metabolic activity, which may reflect surviving cells that are metabolically active but no longer proliferating. In contrast, OFA specifically assesses the ability of surviving cells to proliferate and form PDTO, providing complementary information. Moreover, this assay could allow evaluation of cell population heterogeneity post-irradiation. Investigating the cellular composition of PDTO following different types of irradiation would greatly enhance the biological relevance of the model. In particular, characterizing the subpopulations of cells capable of reforming PDTO after irradiation, so-called Cancer Stem Cells (CSCs), using for example single-cell analyses, could provide valuable insights into the mechanisms of radioresistance. It is acknowledged that CSCs demonstrate an enhanced capacity to initiate PDTO formation [28]. CSCs are considered as a subpopulation of tumor cells with self-renewal and differentiation capabilities, capable of driving tumor initiation, progression, and relapse. They exhibit phenotypic plasticity, allowing dynamic transitions between stem-like and non-stem-like states, which contributes to intratumoral heterogeneity, metastasis, and resistance to treatments [28]. OFA could thus provide evidence for the role of CSCs in radioresistance and support the identification of therapeutic strategies to overcome it. A study on HNSCC cell lines showed that CSC were more capable of proliferation and induced tumorigenicity following irradiation by X-rays or carbon ions [29]. Presence of CSC in the survival fraction of PDTO cells following irradiations would deserve to be further investigated in the future. Moreover, OFA allowed a visual analysis over time combined with quantification. It allows to analyse kinetic over time and requires a small amount of material (300 PDTO per condition), suggesting that this assay could become the new gold standard method to assess radiosensitivity of PDTO.

As expected, viability assay showed that carbon ions exhibited enhanced cell killing efficacy compared to X-rays on PDTO lines derived from HNSCC. Others studies investigated effects of carbon ions on 2D cell lines from HNSCC [4,5,29,30] or on 3D models derived from cell lines [14,15] but this study was the first to use 3D tumor models derived from patients. Interestingly, in 4 out of 5 PDTO lines, we observed a plateau in viability between 4 and 10 Gy of carbon ion irradiation, unexpectedly reaching levels similar to those seen with X-rays. At such high doses, it is likely that cells are over-irradiated, accumulating extensive, unrepaired DNA damage. While these cells are still considered viable according to the ATP assay, they appear unable to repair the damage or to proliferate, as further confirmed by OFA. The RBE calculated using the AUC determined by the viability assay for the 5 lines ranged from 1.14 to 1.94 while RBE calculated using surface occupied by PDTO ranged from 3.14 to 6.54. Clonogenic survival in 2D cell lines remains the classical method to define RBE. However, alternative

approaches have been reported in the literature, such as the evaluation of DNA double-strand break induction [31]. In our study, we chose to estimate RBE using viability assays, which are currently considered the gold standard for assessing treatment response in PDTOs, including in the context of radiotherapy [17]. Although, to our knowledge, this is the first study to estimate RBE using ATP-based viability in cellular models, the values obtained are more consistent to those reported in the literature. Thus, previous results on 2D cells calculated RBE between 2.1 and 2.5 [4,5,32], and the differences observed could be due to the absence of 3D architecture or the lack of heterogeneity. The difference between RBE from the radiosensitive and the radioresistant PDTO line was low when calculated from viability (1.41 vs 1.94) but achieved a higher difference when calculated with OFA at 10 Gy (4.23 vs 6.54).

The results of the cell cycle analysis were globally consistent with viability assay and OFA and tends to support the trends observed in these assays (*i.e* higher efficiency of carbon ions compared to X-rays, and higher differential effect in X-rays-resistant PDTO line), although the results are not strictly overlapping.

In particular, we now address the notable increase in the proportion of S-phase cells in the HN099 model after 10 Gy of carbon ion irradiation (from 6 % in control to 14 % post-irradiation). One hypothesis is that, as shown in the OFA results, the majority of PDTO were eliminated within the 10 days following high-dose CI exposure. This massive reduction in PDTO number may relieve contact inhibition among surviving cells, allowing them to proliferate more freely and re-enter S-phase. Furthermore, immunohistochemistry revealed strong nuclear accumulation of p53 in HN099, suggesting a potential *TP53* mutation (data not shown). This could impair proper cell cycle arrest, allowing cells to continue through the cycle despite DNA damage. The accumulation in S-phase could also reflect replication stress or checkpoint slippage [33]. Finally, high proportion of sub-G1 events in these conditions indicates extensive cell death, which may affect the relative distribution of the remaining viable cells across the different cell cycle phases. Another notable discrepancy lies in the lower sub-G1 fraction observed in HN065 PDTOs following 10 Gy of carbon ion irradiation compared to the same dose of X-rays (40.5 % vs. 49.91 %). This difference may stem from the higher biological effectiveness of carbon ions, which induce early apoptosis that may evolve into late apoptosis or necrosis over the course of 10 days. Consequently, this could lead to a reduced detection of apoptotic bodies, even though the Organoid Formation Assay (OFA) reveals a stronger inactivating effect of 10 Gy carbon ion irradiation compared to X-rays. Moreover, the blockage in G2/M cell cycle progression observed in the sensitive PDTO line is quite similar following X-rays and carbon ion exposures and there was no blockage in G2/M in the resistant PDTO line. Those results differed from other studies on 2D cell lines where blockage in G2/M was more important in radioresistant cell lines than in sensitive cell lines [30,34,35]. However, those conclusions were based on analysis of the cell cycle 24 h after irradiation. In one of those studies, for the cell line that displayed a strong increase of cells in G2-M phase 24 h post-irradiation [30], they showed a decreased of this proportion 10 days post-irradiation, suggesting that after this delay the blockage in the cell cycle was overcome by the cells. A limitation of our study is thus the timing of the post-irradiation analyses for cell cycle and cell death. Due to restricted access to sufficient biological material at earlier timepoints, these assays were performed later than the optimal window for capturing immediate radiation-induced effects, such as early G2-M arrest or apoptosis. As a result, the observed differences in cell cycle distribution and sub-G1 fractions were relatively modest and may not fully reflect the early cellular responses to irradiation. It is worth noting that sensitivity to X-rays among the PDTO lines is not associated with higher proliferation rate, as the radioresistant model actually exhibited a slightly higher proliferation rate than the radiosensitive one (data not shown). We thus showed that the X-ray-sensitive PDTO line was more sensitive to carbon ions, but the most interesting part was that the X-ray-resistant PDTO line was almost four times more sensitive to carbon ions compared to X-rays. This observation reinforces the idea that carbon ions could be especially beneficial for patients with X-ray-resistant tumors. Future research should aim to validate this finding in a larger panel of resistant models and to decipher the underlying mechanisms, which could ultimately guide patient selection for hadrontherapy.

A phase II prospective study showed therapeutic effectiveness of carbon ions on 236 patients with head and neck cancers but most of them were patients with rare tumours and only a few patients had HNSCC [3]. Other clinical studies on head and neck cancers are ongoing but only a few focused on HNSCC [36]. The use of carbon ions in clinic is still limited because this technology is expensive and only a few centres exist worldwide, preventing its routine development. In this context, we showed that PDTO seem to be relevant models to study the biological effects of carbon ions. It is now essential to expand the panel models tested for irradiations to perform meaningful subgroup analysis and identify predictive biomarkers susceptible to select profiles of tumours sensitive to carbon ions and design further clinical trials. The first carbon ions beam facility for treatment in France will be available by 2025 [37] and identifying patients who will benefit the most from this costly technology is crucial. Thus, development of predictive functional assays based on PDTO could help to identify patients who could benefit from carbon ions.

Conclusion

These results showed the feasibility of irradiating PDTO with carbon ions and assessing their response at the individual level using multiple assays. OFA appeared as a relevant method to evaluate survival and regrowth capacity, enabling comparison of different radiotherapy modalities and RBE calculation.

Interestingly, the X-ray-resistant PDTO line showed a strong sensitivity to carbon ions. This finding warrants further investigation into the underlying mechanisms and suggests that carbon ion therapy may help overcome resistance to conventional radiotherapy in HNSCC, opening new perspectives for improving treatment strategies and ultimately enhancing patient care.

CRediT authorship contribution statement

Marion Perréard: Writing – original draft, Investigation, Visualization, Formal analysis, Funding acquisition. **Romane Florent:** Writing – review & editing, Investigation. **Jordane Divoux:** Investigation, Writing – review & editing. **Vianney Bastit:** Investigation, Writing – review & editing. **Lucie Lecouflet:** Investigation. **Guillaume Desmartin:** Investigation. **Sterenn Guillemot:** Formal analysis. **Léonie Ibazizene:** Investigation. **Nicolas Elie:** Methodology. **Emilie Brotin:** Resources. **Laurent Poulain:** Supervision, Writing – review & editing, Conceptualization. **Emmanuel Babin:** Supervision. **Juliette Thariat:** Writing – review & editing, Conceptualization. **François Chevalier:** Investigation, Writing – review & editing, Resources, Conceptualization. **Louis-Bastien Weiswald:** Supervision, Validation, Funding acquisition, Writing – original draft, Investigation, Conceptualization.

Funding

The authors would like to acknowledge funding from Groupement des Entreprises Françaises dans la lutte contre le Cancer (GEFLUC) of Normandie, from Fonds de dotation Patrick Brou de Laurière (CD 48/FDPBL/2021) and from Ligue Contre le Cancer. This work is part of the "ORGATHEREX" European project, co-funded by the Normandy County Council, the European Union within the framework of the Operational Program ERDF/ESF 2014–2020.

Declaration of competing interest

The authors declare that they have no known competing financial interests or personal relationships that could have appeared to influence

the work reported in this paper.

Acknowledgements

Irradiations with Carbon Ions were performed at GANIL, France, using beam time obtained under experiment number P1369-H of the iPAC 2023 call. The CIRIL-GANIL dosimetry team and beam operators are acknowledged for extensive support. The authors would like to thank Maryline Guillamin (IsoCELL core facility, Service Unit PLATON, University of Caen Normandie), Florence Giffard (VIRTUAL'HIS core facility, Service Unit PLATON, University of Caen Normandie) for their helpful technical support, and Christophe Denoyelle (ImpedanCELL core facilty, Service Unit PLATON, University of Caen Normandie) for real-time imaging experiments. The IncuCyte S3 device was acquired thanks to the support of the French State and the 'Normandy County Council' (Contrat de Plan Etat Région – CPER INNOVONS). We are grateful to Jérôme Toutain (Cyceron core facility, University of Caen) for X-ray experiments. The ORGAPRED project is co-funded by the Normandy County Council, the European Union within the framework of the Operational Programme ERDF/ESF 2014–2020 which was conducted as part of the planning contract 2015–2020 between the French State and the Normandy Region.

Author's contributions

MP and LBW wrote the manuscript. MP, EB, LP, JT, FC and LBW devised the study concept and design. MP, RF, JD, LI, VB, LL, GD, FC and LBW carried out the experiments. SG, NE, and EB contributed to the interpretation of the results. Each author read and approved the final manuscript and has been sufficiently involved in the work to take public responsibility for appropriate portions of the content. Figures and illustrations were designed and created by MP. Funding was obtained by LBW.

Appendix A. Supplementary data

Supplementary data to this article can be found online at https://doi.org/10.1016/j.radonc.2025.111026.

References

[1] Sacco AG, Cohen EE. Current treatment options for recurrent or metastatic head and neck squamous cell Carcinoma. J Clin Oncol 2015;33:3305–13.
[2] Ngamphaiboon N, Chairoungdua A, Dajsakdipon T, Jiarpinitnun C. Evolving role of novel radiosensitizers and immune checkpoint inhibitors in (chemo)radiotherapy of locally advanced head and neck squamous cell carcinoma. Oral Oncol 2023;145:106520.
[3] Mizoe JE, Hasegawa A, Jingu K, Takagi R, Bessyo H, Morikawa T, et al. Results of carbon ion radiotherapy for head and neck cancer. Radiother Oncol 2012;103:32–7.
[4] Belli M, Bettega D, Calzolari P, Cherubini R, Cuttone G, Durante M, et al. Effectiveness of monoenergetic and spread-out bragg peak carbon-ions for inactivation of various normal and tumour human cell lines. J Radiat Res 2008;49:597–607.
[5] Beuve M, Alphonse G, Maalouf M, Colliaux A, Battiston-Montagne P, Jalade P, et al. Radiobiologic parameters and local effect model predictions for head-and-neck squamous cell carcinomas exposed to high linear energy transfer ions. Int J Radiat Oncol Biol Phys 2008;71:635–42.
[6] Borrell B. How accurate are cancer cell lines? Nature 2010;463:858.
[7] Poh WT, Stanslas J. The new paradigm in animal testing - "3Rs alternatives". Regul Toxicol Pharm 2024;153:105705.
[8] Weiswald LB, Bellet D, Dangles-Marie V. Spherical cancer models in tumor biology. Neoplasia 2015;17:1–15.
[9] Mery B, Rancoule C, Guy JB, Espenel S, Wozny AS, Battiston-Montagne P, et al. Preclinical models in HNSCC, a comprehensive review. Oral Oncol 2017;65:51–6.
[10] Tschachojan V, Schroer H, Averbeck N, Mueller-Klieser W. Carbon ions and X-rays induce pro-inflammatory effects in 3D oral mucosa models with and without PBMCs. Oncol Rep 2014;32:1820–8.
[11] Nowrouzi A, Sertorio MG, Akbarpour M, Knoll M, Krunic D, Kuhar M, et al. Personalized assessment of Normal tissue radiosensitivity via transcriptome response to photon, proton and Carbon irradiation in patient-derived human intestinal organoids. Cancers (Basel) 2020;12.
[12] Hamdi DH, Chevalier F, Groetz JE, Durantel F, Thuret JY, Mann C, et al. Comparable senescence induction in three-dimensional human Cartilage model by exposure to therapeutic doses of X-rays or C-ions. Int J Radiat Oncol Biol Phys 2016;95:139–46.
[13] Sekihara K, Himuro H, Saito N, Ota Y, Kouro T, Kusano Y, et al. Evaluation of X-ray and carbon-ion beam irradiation with chemotherapy for the treatment of cervical adenocarcinoma cells in 2D and 3D cultures. Cancer Cell Int 2022;22:391.
[14] Roohani S, Loskutov J, Heufelder J, Ehret F, Wedeken L, Regenbrecht M, et al. Photon and proton irradiation in patient-derived, three-dimensional soft tissue Sarcoma models. BMC Cancer 2023;23:577.
[15] Charalampopoulou A, Barcellini A, Peloso A, Vanoli A, Cesari S, Icaro Cornaglia A, et al. Unlocking the potential role of Decellularized biological scaffolds as a 3D radiobiological model for low- and high-LET irradiation. Cancers (Basel) 2024;16.
[16] Thorel L, Perreard M, Florent R, Divoux J, Coffy S, Vincent A, et al. Patient-derived tumor organoids, a new avenue for preclinical research and precision medicine in oncology. Exp Mol Med 2024;56:1531–51.
[17] Driehuis E, Kolders S, Spelier S, Lohmussaar K, Willems SM, Devriese LA, et al. Oral mucosal organoids as a potential platform for personalized cancer therapy. Cancer Discov 2019;9:852–71.
[18] Millen R, De Kort WWB, Koomen M, van Son GJF, Gobits R, Penning de Vries B, et al. Patient-derived head and neck cancer organoids allow treatment stratification and serve as a tool for biomarker validation and identification. Med 2023;4:e12.
[19] Lee DW, Choi SY, Kim SY, Kim HJ, Shin DY, Shim J, et al. A novel 3D pillar/well array platform using patient-derived head and neck tumor to predict the individual radioresponse. Transl Oncol 2022;24:101483.
[20] Perreard M, Florent R, Divoux J, Grellard JM, Lequesne J, Briand M, et al. ORGAVADS, establishment of tumor organoids from head and neck squamous cell carcinoma to assess their response to innovative therapies. BMC Cancer 2023;23:223.
[21] Durantel F, Balanzat E, Cassimi A, Chevalier F, Ngono-Ravache Y, Madi T, et al. Dosimetry for radiobiology experiments at GANIL. Nucl Instrum Methods Phys Res, Sect A 2016;816:70–7.
[22] Schindelin J, Arganda-Carreras I, Frise E, Kaynig V, Longair M, Pietzsch T, et al. Fiji, an open-source platform for biological-image analysis. Nat Methods 2012;9:676–82.
[23] Lowe DG. Distinctive image features from scale-Invariant keypoints. Int J Comput Vis 2004;60:91–110.
[24] Franken NA, Rodermond HM, Stap J, Haveman J, van Bree C. Clonogenic assay of cells in vitro. Nat Protoc 2006;1:2315–9.
[25] Serrano-Mendioroz I, Garate-Soraluze E, Rodriguez-Ruiz ME. A simple method to assess clonogenic survival of irradiated cancer cells. Methods Cell Biol 2023;174:127–36.
[26] Charpentier M, Bloy N, Formenti SC, Galluzzi L, Demaria S. Live imaging to quantify Cellular radiosensitivity in patient-derived tumor organoids. J Vis Exp 2024.
[27] Lee DW, Lee SY, Park L, Kang MS, Kim MH, Doh I, et al. High-throughput clonogenic analysis of 3D-cultured patient-derived cells with a Micropillar and microwell Chip. SLAS Discov 2017;22:645–51.
[28] Loh JJ, Ma S. Hallmarks of cancer stemness. Cell Stem Cell 2024;31:617–39.
[29] Bertrand G, Maalouf M, Boivin A, Battiston-Montagne P, Beuve M, Levy A, et al. Targeting head and neck cancer stem cells to overcome resistance to photon and carbon ion radiation. Stem Cell Rev Rep 2014;10:114–26.
[30] Maalouf M, Alphonse G, Colliaux A, Beuve M, Trajkovic-Bodennec S, Battiston-Montagne P, et al. Different mechanisms of cell death in radiosensitive and radioresistant p53 mutated head and neck squamous cell carcinoma cell lines exposed to carbon ions and x-rays. Int J Radiat Oncol Biol Phys 2009;74:200–9.
[31] Frese MC, Yu VK, Stewart RD, Carlson DJ. A mechanism-based approach to predict the relative biological effectiveness of protons and carbon ions in radiation therapy. Int J Radiat Oncol Biol Phys 2012;83:442–50.
[32] Feng H, Li W, Zhang Y, Chang C, Hua L, Feng Y, et al. Mechanistic modelling of relative biological effectiveness of carbon ion beams and comparison with experiments. Phys Med Biol 2024;69.
[33] Benedict B, van Harn T, Dekker M, Hermsen S, Kucukosmanoglu A, Pieters W, et al. Loss of p53 suppresses replication-stress-induced DNA breakage in G1/S checkpoint deficient cells. Elife 2018;7.
[34] Wozny AS, Alphonse G, Cassard A, Malesys C, Louati S, Beuve M, et al. Impact of hypoxia on the double-strand break repair after photon and carbon ion irradiation of radioresistant HNSCC cells. Sci Rep 2020;10:21357.
[35] Luo H, Yang Z, Zhang Q, Shao L, Wei S, Liu R, et al. Carbon Ion therapy inhibits esophageal squamous cell Carcinoma metastasis by upregulating STAT3 through the JAK2/STAT3 signaling pathway. Front Public Health 2020;8:579705.
[36] Zhang W, Kong L, Lu JJ. A cross-sectional analysis of registered clinical trials on the use of particle beam radiation therapy in head and neck cancers. Ann Transl Med 2022;10:1192.
[37] Chevalier F, P. L, and Gaubert G. CYCLHAD. A french facility dedicated for Research and treatment in hadrontherapy. Nucl Phys News 2022;32:27–31.